Experimental study of the spatial resolution of silicon microstrip detectors for the Inner Tracking System of the ALICE Detector

L. Arnold, J.P. Coffin, P. Fintz, G. Guillaume, F. Jundt, C. Kuhn,
J.R. Lutz, P. Pagès, S. Pozdniakov, F. Rami, K. Šparavec, L. Tizniti

Institut de Recherches Subatomiques [1], IN2P3-CNRS/ULP - BP28
67037 Strasbourg Cedex, France

C. Colledani, W. Dulinski, R. Turchetta

LEPSI - BP28
67037 Strasbourg Cedex, France

C. Roy

SUBATECH
Ecole des Mines de Nantes
44070 Nantes Cedex 03, France

Abstract

Tests of Silicon-Strip detectors are currently performed in the framework of the design and the construction of the two outer layers of the Inner Tracking System (ITS) of the ALICE detector. The physics signal treatment and cluster finding for some detectors tested with a ^{90}Sr β-source on a test bench and with a 10 GeV pion beam from the Proton Synchrotron (PS) at CERN are presented. The tracking procedure and the determination of the resolution of these detectors using the pion beam are described. The spatial resolution of two single-sided detectors with a relative stereo angle of 35 mrad between them is found to be equal to 6 μm.

---

[1]On May 1st, 1997, the "Centre de Recherches Nucléaires" (CRN) becomes the "Institut de Recherches Subatomiques" (IReS)

1   Introduction

This note aims at the description of the procedure followed to measure the spatial resolution of microstrip detectors. It enters in the framework of R&D activities devoted to the design of the two outer layers of the ALICE detector.

A description of the tested microstrip detectors, their characteristics and their expected performances is given. It is followed by the description of the experimental setups that have been used for the tests both at IReS-Strasbourg and CERN. The analysis of the collected information is then described, with emphasis on the charge cluster extraction, the track reconstruction, and the measurement of the spatial resolution of the detector by using the experimental setup at CERN . Some conclusions and perspectives are presented.

2   The microstrip detectors for the ALICE experiment

2.1   General description

Silicon microstrip detectors will equip the two outer layers of the ITS (Inner Tracking System) of the ALICE detector. These layers will be crucial for connecting the tracks between the ITS and the TPC (Time Projection Chamber) located around the ITS. They will also provide dE/dx information for charged particle identification.

The two outer layers of the ITS are designed as modules of approximately 75 mm × 42 mm, with a thickness of 300 μm. Each module contains a double-sided detector with the front-end electronics, coupling capacitors, bias circuits and cabling. These modules are glued on a carbon fibre support, forming the basic ITS ladder structure.

In order to obtain an optimal resolution in the bending plane, the strips will be oriented parallel to the beam direction (z axis). In this way, the $r\varphi$ resolution is essentially fixed by the pitch of the strips, taken as 95 μm, giving an expected resolution of 30 μm [1]. With a stereo angle of 35 mrad between the two plans of microstrip detectors, a resolution of 860 μm is expected in the z direction.

In the ALICE technical proposal [1], double-sided silicon strip detectors are proposed to be used. The major interest of this choice is that, beside a reduced radiation length with respect to two single-sided detectors, a double-sided detector allows the matching of the charge signals collected on the two sides and reduces the ambiguities due to multiple hits [2, 3]. It also presents some drawbacks like a non trivial signal readout.

2.2   Characteristics of the tested detectors

As a first campaign of measurements, we use, in the present study, single-sided detectors of 20 × 20 mm, the pitch is 50 μm and the thickness 300 μm. These detectors are tested by pairs, but kept independent (not glued together). Two different pairs of detectors were used:

- The detectors of the first pair count 384 strips each, the strips of one detector being oriented orthogonally to those of the other. These detectors have also intermediate strips, not connected but collecting charges by capacitive coupling. These detectors were tested by using a ^{90}Sr β-radioactive source on a test bench mounted at the IReS-Strasbourg;

- The second pair consists of detectors of 356 strips each, the strips of one detector having a relative stereo angle of 35 mrad with the strips of the other detector. Intermediate

strips are also existing between the readout strips. These detectors were tested by using a 10 GeV pion beam from the Proton Synchrotron at CERN.

Two different Viking Amplifier readout electronics (VA1 and VA2) are associated respectively with each pair of detectors.

To avoid ambiguities, we give, in Fig.1, the correspondence between the $(r\varphi,z)$ coordinates used in the ALICE technical proposal and the (x,y,z) coordinates used in this study:
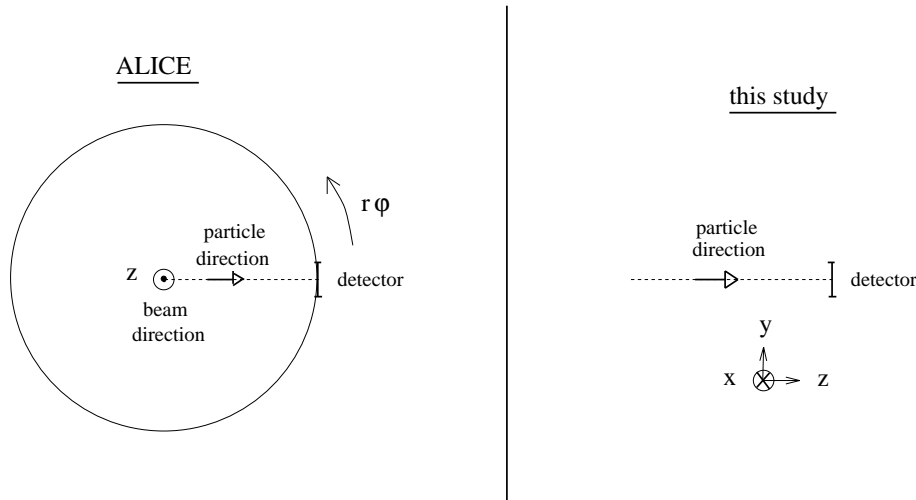

Figure 1: Correspondence between the $(r\varphi,z)$ coordinates used in the ALICE technical proposal and the (x,y,z) coordinates used in this study.

3   Experimental setups

A brief description of the two experimental setups used in this study is given in the next two paragraphs.

3.1   Test bench at IReS-Strasbourg

The experimental setup is shown in Fig.2. It consists of a collimated radioactive source, two scintillators read by photomultipliers defining a trigger and a rotatable box with the two tested detectors.

Data control and acquisition are performed by VME electronic modules for the analog/digital data conversion. The online data acquisition is based on the MicroDAS programs, using OS9 system, implemented by the LEPSI group in Strasbourg.

3.2   Detector bench at CERN

The telescope of detectors used at CERN is sketched in Fig.3. It consists of four pairs of reference detectors (called X_i and Y_i, with i=1 to 4) and one pair of detectors (Y_5 and Y_6) to be tested, with a relative stereo angle of 35 mrad between their strips. The tested detectors are placed upstream of the set of reference detectors. This, of course, does not correspond to an ideal location for such tests. It was, however, the only convenient way to study these silicon microstrip detectors within the framework of an experiment devoted to other purposes.
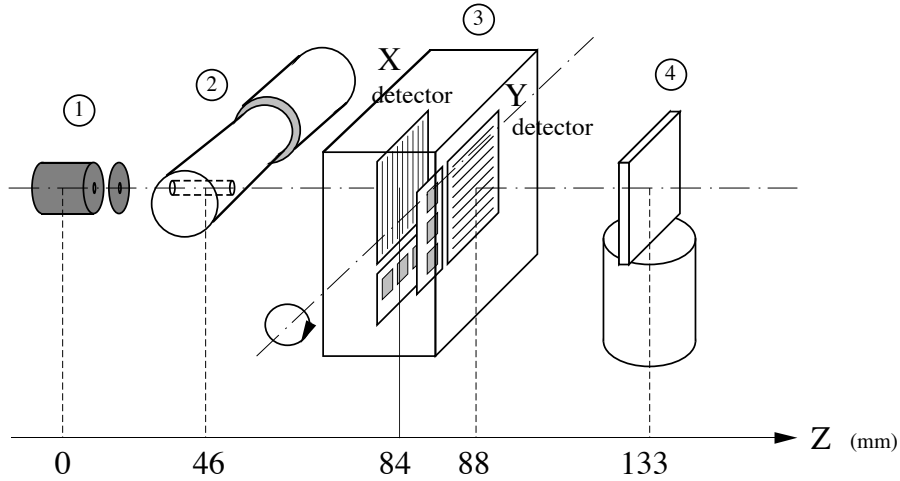
Figure 2: General view of the test bench at IReS-Strasbourg. (1) radioactive source, (2) scintillator used as an active collimator read by a photomultiplier, (3) rotatable box containing the two tested detectors, (4) scintillator read by a photomultiplier. The lower scale indicates the relative position of the different elements with respect to the source, used as the origin.
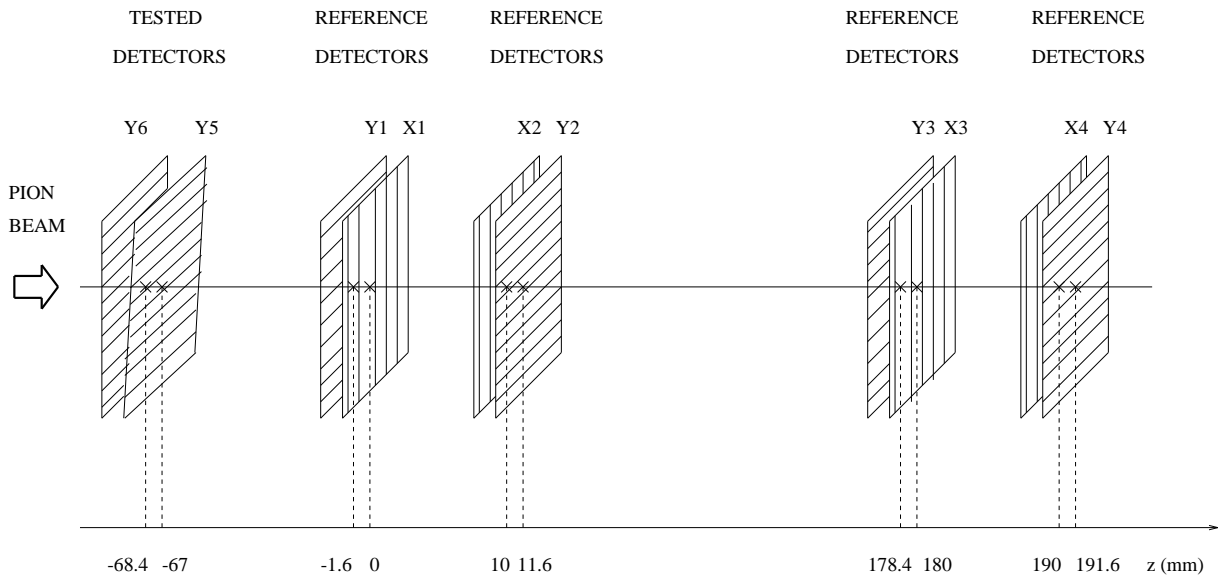

Figure 3: Detector telescope used with a pion beam. The relative positions of the different detectors are reported (in mm) with respect to the X_1 detector, used as the origin.

4   Charge cluster reconstruction

In this section and the next, details are given about the analysis of the collected data with either of the two experimental setups. This analysis is based on a computer program initially developed by R. Turchetta [4].

First, we describe how the signal is determined from the raw data. This is done by subtracting the pedestal and the common mode shift from them. The sequential calculation of the pedestal, the common mode shift and the signal is given in paragraph 4.1 together with the calculation of the residual noise, useful to determine the signal/noise ratio itself needed when looking for charge clusters. In paragraph 4.2, the description of the criteria used for the cluster determination is given, as well as the determination of the mean position of these clusters.

4.1   Pedestal, common mode shift, noise and signal determination

When a particle passes through a detector, defining an event, the corresponding ADC count number can be divided in three parts, and may be written as follows:

$$ADC(i,k) = P(i,k) + D(k) + S(i,k),$$

where i is the strip number and k the event number.

$P(i,k)$ is the *pedestal* which fluctuates around a baseline. These fluctuations are due to electronic non uniformities of each readout channel (1 channel/strip).

$D(k)$ is the *common mode shift*, resulting from an electronic parasite pick-up which is specific to each chip and varies with time.

$S(i,k)$ represents the signal plus the residual noise and is deduced from $ADC(i,k)$, $P(i,k)$ and $D(k)$.

These quantities are calculated in the following order:

1. The initial pedestal value is the first quantity to be extracted. It is defined as the mean value of the ADC counts over a given number of initial events, taken equal to 200. It allows a smoothing of the successive values which remains unchanged when a larger number of events is considered. This initial value of the pedestal will allow for determining all the other quantities for the remaining events. It reads:

$$P(i,200) = \frac{1}{200} \sum_{k=1}^{200} ADC(i,k). \tag{1}$$

2. For any event following the first 200's, the common mode shift is calculated for each electronic chip as the mean ADC count number whose the pedestal of the preceding event is subtracted from:

$$D(k) = \frac{1}{128} \sum_{i=1}^{128} [\, ADC(i,k) - P(i,k-1) \,] \,, \tag{2}$$

where $k > 200$.

3. For each event, the pedestal value is given by a recurrent formula depending on the pedestal value of the preceding event:

$$P(i,k) = \frac{1}{W_p} \cdot \{\, [W_p - 1]\, P(i,k-1) + ADC(i,k) - D(k) \,\}, \tag{3}$$

where W_p is a weight chosen equal to 100 (see details below).

4. The signal is extracted as:

$$S(i,k) = ADC(i,k) - P(i,k) - D(k). \tag{4}$$

The charge cluster finding which will be described in the next paragraph, requires the signal/noise ratio determination for each strip of the detector. The noise is calculated in two steps:

- An initial value is defined as the mean dispersion of the signal values for a given number of events, taken here equal to 200, following the first 200 events, by using the following relationship:

$$N(i, 400) = \left\{ \frac{\sum_{k=201}^{400}[ADC(i,k)]^2}{200} - \left[\frac{\sum_{k=201}^{400}[ADC(i,k)]}{200} \right]^2 \right\}^{1/2} . \tag{5}$$

- The noise is then computed for all the remaining events as:

$$N(i, k) = \frac{1}{W_n} \cdot \left\{ \, [W_n - 1] \, [N(i, k-1)]^2 + [S(i,k)]^2 \, \right\}^{1/2} , \tag{6}$$

where $k > 400$ and W_n is a weight chosen equal to 100.

In the recurrent formulas 3 and 6, the pedestal and the noise of a given event are calculated by using the pedestal and the noise of the preceding event. To express that the difference of the pedestal (or the noise) between two successive events corresponds to a small fluctuation, we use the term $(W_p - 1)/W_p$ (or $(W_n - 1)/W_n$).

The weights were taken as $W_p = 100$ and $W_n = 100$ in such a way that they are low enough to smooth out weak fluctuations and to take into account seldom larger fluctuations.
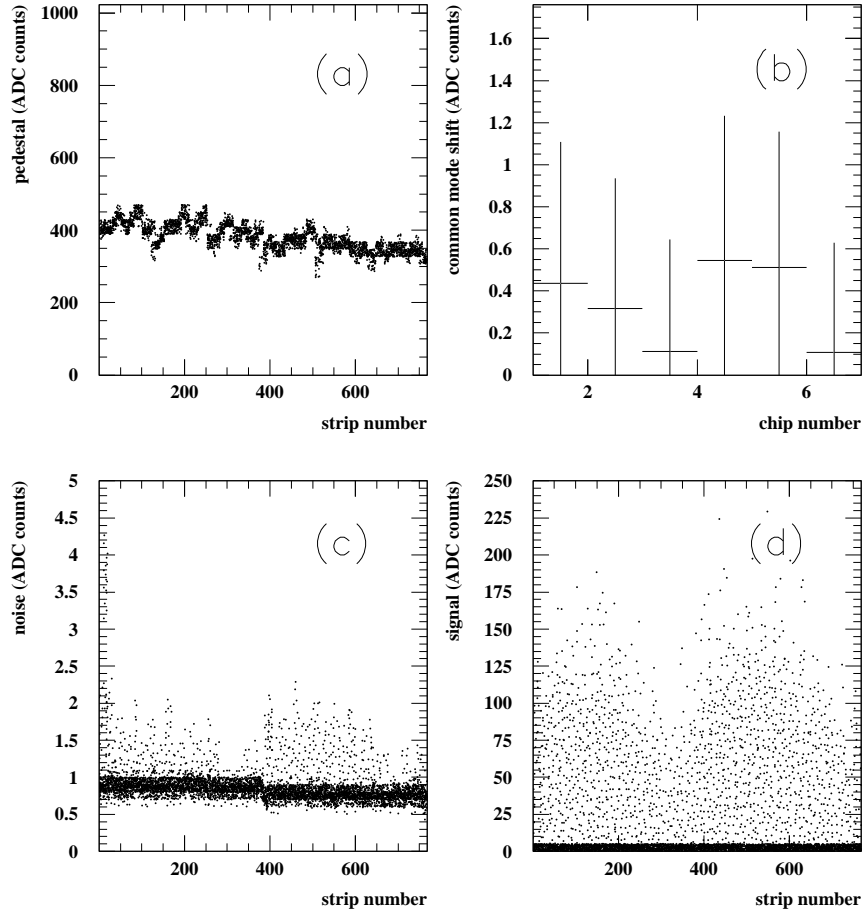

Figure 4: (a) Pedestal, (b) Common mode shift, (c) Noise and (d) Signal obtained, using the ^{90}Sr β-source, for a total of 10^4 events.

4.2 Cluster finding algorithm

The aim of the cluster finding algorithm is to select the strips which are concerned by the passage of a particle. They correspond to the strips with the higher signal/noise ratio. The cluster finding criteria are described in paragraph 4.2.1. Having found clusters, their mean position is determined using an algorithm presented in paragraph 4.2.2.

4.2.1 Selection of clusters

After extraction from the initial raw data of the pedestal and the common mode shifts, the only available variables to be used for the selection of clusters are the signal and the noise. The cluster selection criteria will thus be defined by using these two variables and their ratio by applying on them different thresholds.

This selection operates in the following steps:

1. The strips are examined by pairs which are retained if the noise of the strips of the pair ranges between 0.1 and 8 ADC counts and if the sum of their signal/noise ratio is larger than 4,

2. The cluster existence is examined on the basis of the first strip of the selected pair plus 5 strips on each side,

3. The central strip of each cluster (i.e. the strip with the highest signal/noise ratio) must have a signal/noise ratio larger than 20. The neighbouring strips (i.e. the strips located on both sides of the central strip) are kept if their signal/noise ratio exceeds 8. If one of the examined strips has a signal/noise ratio lower than 8, the treatment is stopped and the remaining strips are not retained,

4. The charge cluster signal is defined as the sum of the individual signals, and the cluster signal/noise ratio as the sum of the signal/noise ratios of all concerned strips. The cluster is finally retained if its signal ranges between 5 and 1000 ADC counts, its signal/noise ratio exceeds 20 and the number of strips is less than 5.

The thresholds applied to the noise and signal have been adjusted knowing that the noise values are typically of 1 ADC count (Fig.4 (c)) when using the ^{90}Sr source and 2.5 ADC counts for the pion beam. The values for the signals go up to 200 ADC counts in the first case (Fig.4 (d)) and up to 1000 ADC counts in the second.

Fig.5 shows the distribution of the number of strips per cluster, obtained in the case of the pion beam and of the ^{90}Sr source. It shows that the mean number of hit strips is respectively 2.20 and 2.72, which means that the charge is generally distributed over two strips. Nevertheless, these numbers may be affected by the contribution of cross-talk between the strips and other electronic sources. Moreover, this number is higher if the ^{90}Sr source is used. This is explainable by some contribution of the multiple scattering of the low energy electrons into the detector and the surrounding material upstream.

Fig.6 illustrates the cluster signal/noise ratio by using both the pion beam and the ^{90}Sr source. Large ratios are obtained in both cases.

4.2.2 Determination of the mean cluster position

The mean cluster position is determined from the variable η which is defined for each pair of strips as:

$$\eta = S_R/(S_L + S_R),$$

where S_L and S_R are the signals measured respectively on the left and the right strip of a pair.
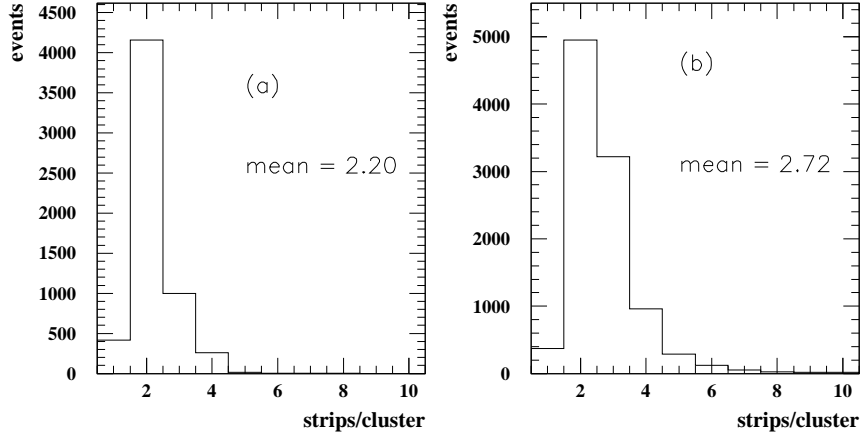
Figure 5: Number of strips per cluster using (a) the 10 GeV pion beam and (b) the collimated ^{90}Sr source.
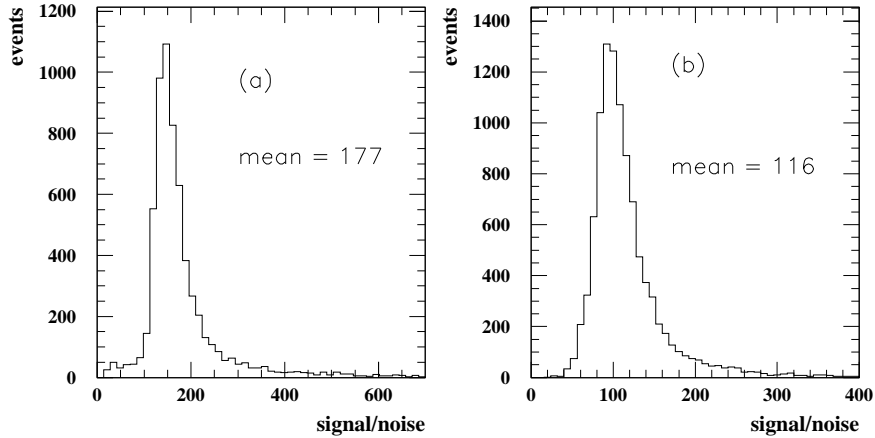

Figure 6: Distribution of the signal/noise ratio of the reconstructed clusters for a total of 10^4 events by using (a) the 10 GeV pion beam and (b) the ^{90}Sr source.

For a given value of η, we associate a function defined for 100 bins ranging from 0 up to 1, according to:

$$f(\eta_0) = \frac{\int_0^{\eta_0} \frac{dN}{d\eta} d\eta}{\int_0^1 \frac{dN}{d\eta} d\eta} \ ,$$

where $\frac{dN}{d\eta}$ gives the differential η distribution, and η_0 is the mean value of each of the 100 bins.

The mean cluster position (expressed in strip number) is given by:

$$P_{mean} = P_1 + f(\eta),$$

where P_1 is the central strip if the signal/noise ratio of the strip at the right side of the central strip is higher than the signal/noise ratio of the strip at its left side and P_1 is the central strip $-$ 1 otherwise. η is calculated by using the strips P_1 and the strip situated on its right.

The mean cluster position in strip number P_{mean} is then converted into millimeters with the following relation:

$$y_{mean} = [\ (P_{cent} - P_{first} \ ) \ \epsilon + offset \ ] \cdot pitch,$$

8

where	P_{first}	is the number of the first strip of the detector,
	ϵ	is the reading direction,
	$offset$	is an offset due to the choice of the origin,
and	$pitch$	is the detector pitch (50 μm).

The η distribution obtained both for the pion beam and the ^{90}Sr source is shown in Fig.7 .

In the case of the pion beam (a), the distribution is characterized by two peaks around the values 0 and 1 and a third peak around 0.5 . The first two maxima show that nearly only one strip collects the majority of the cluster charges. This is due to the fact that pions cross orthogonally the detector and the multiple scattering is weak. The peak around 0.5 is due to the intermediate strips, read out by capacitive effect (no voltage is applied on these strips).

In the case of the ^{90}Sr source (b), one observes a broad distribution peaking around 0.5. This results from the multiple scattering of the electrons which has been already mentioned, as well as from a non well-defined "electron beam" despite the source collimation.
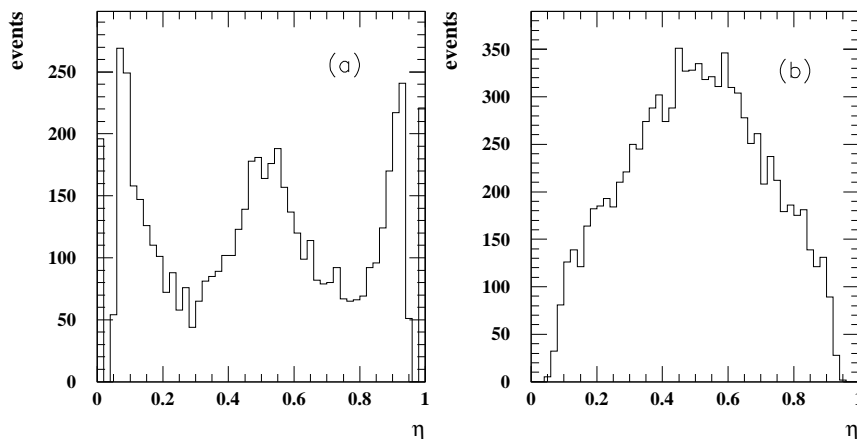

Figure 7: Distribution of the η variable as measured (a) with the 10 GeV pion beam, and (b) with the ^{90}Sr source.

5   Track reconstruction and measurement of the detector resolution

In this section, the track reconstruction is described together with the determination of the tested detector resolutions. Here, only detectors exposed to the 10 GeV pion beam are considered.

As we deal with adjustments of the order of some μm's – quasi-impossible to obtain in the relative positioning of the telescope detectors – a careful alignment of the different detectors has to be made by software.

First, a prealignment of detectors is performed and consists of a fictive vertical translation of all the detectors of the telescope (paragraph 5.1). After track determination by using a χ^2 minimization method (paragraph 5.2), the alignment of detectors is performed and consists of a fictive relative rotation of the detectors (paragraph 5.3). It is then possible to extract the spatial resolution by comparing the fitted and reconstructed track position coordinates (paragraph 5.4). Finally, the effects of the multiple scattering and of the variation of the track incident angle on the resolution are discussed (paragraphs 5.4.2 and 5.5).

5.1 Prealignment of detectors

The prealignment of all detectors requires to take one of them as a reference : in this study, the detector 1 is chosen as such. Then, the distribution of the difference between the coordinates of the mean cluster position of any detector and of the reference detector is calculated. If the detector is vertically misaligned as compared to the reference detector, the distribution is not centered on 0. The offset is given by the shift of the mean value of the distribution with respect to 0.

5.2 Tracking procedure description

The reference detectors 1, 2, 3 and 4 (Fig.3) are used to reconstruct the tracks from the corrected coordinates. This is done by using a χ^2 minimization method, with:

$$\chi^2 = \sum_{i=1}^{4} \frac{1}{\sigma_i^2} \left(u_i^{meas} - a - b \; z_i \right)$$

where i is running on all the reference detectors,
σ_i is the resolution of the detector i (taken as 1.5 μm),
u_i^{meas} is the measured cluster mean position ($u_i{=}x_i$ or y_i),
a and b are the track parameters,
and z_i is the z position of the detector i.

Finally, this allows the linear track determination for all detectors (reference and tested) as:

$$\begin{cases} x^{fit} = a_x + b_x \; z \\ y^{fit} = a_y + b_y \; z \; . \end{cases}$$

The fitted tracks are accepted if only one cluster is found in each reference detector. This means that events in which no cluster or more than one cluster is found for at least one reference detector are rejected. Moreover, this condition must be fulfilled for both X and Y directions.

5.3 Alignment of detectors

Only (x, z) and (y, z) translations have been considered at this point. It is also essential to bring all detector strips parallel to those of the initial reference detector. These angular corrections constitute the alignment of detectors.

The alignment angles obtained in this study are 14 and 65 mrad, respectively, for detectors 5 and 6. In case of detector 6, the obtained value contains also the contribution of the required stereo angle of 35 mrad (paragraph 2.2). The alignment angle for this detector is thus in fact 30 mrad.

5.4 Determination of the detector spatial resolution

The y coordinates, measured by using the two tested detectors and called y_5 and y_6 are used to determine the x coordinate according to the relation:

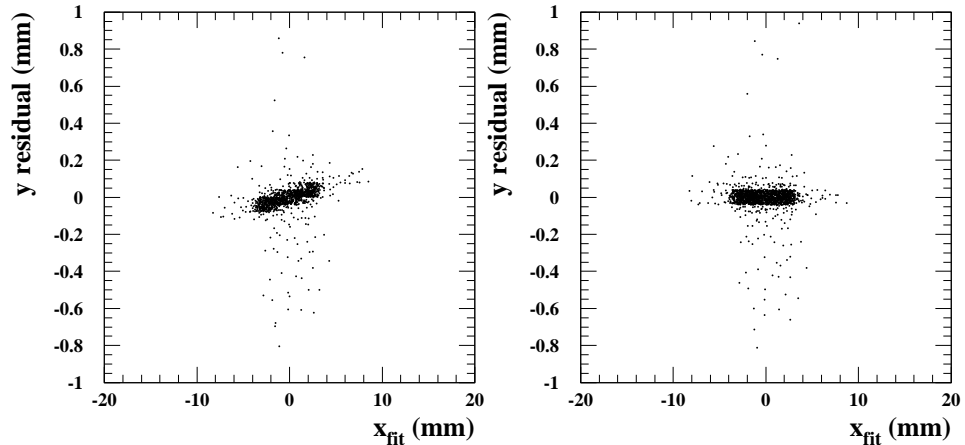$$x = \frac{y_5}{\tan(35 \; mrad)} - \frac{y_6}{\sin(35 \; mrad)} \; .$$

Figure 8: y residual as a function of x^{fit} for detector 5 (a) before and (b) after the alignment of detectors.

To obtain the resolution (in both the x and y directions), we consider the distribution of the difference between the fitted and measured positions, also called *residual*. The resolution is defined as:

$$\sigma = \left\{ \sigma_{resid}^2 - \sigma_{ms}^2 \right\}^{1/2} , \tag{7}$$

where σ_{resid} is the width of the gaussian which is fitted on the distribution of residuals, and σ_{ms} is the contribution of the multiple scattering.

The determination of these two contributions to the resolution is given in the following two paragraphs.

5.4.1 Determination of the x and y residual widths

After alignment, the y residual width is found equal to 18 μm.

It should be emphasized that this measurement is obtained by considering the detector configuration given on Fig.3, where the tested detectors are placed upstream the reference telescope. A better choice would be, of course, to insert these detectors in between the reference detectors.

To investigate this effect in the case of the present configuration, it is possible to use the detector 6 as a reference detector, i.e. to include it in the fitting procedure. Then, the y residual width reduces down to 7.1 μm.

Other detector configurations may also be considered. Table 1 summarizes the results of different configurations. One sees, for example, that by using detectors 3 and 4 as tested detectors, the large distance from the other detectors degrades their y residual width from 3 μm to about 30 μm.

This explains the relatively high value of the y residual width obtained for the tested detectors 5 and 6, and suggests that the actual value is in fact in the domain of only some units of μm.

The x residual width was found to be 230 μm.

Fig.9 shows the y and x residual distributions of the tested detectors. These are fitted with a gaussian function whose width is also given.

In Fig.10, the residual distribution of the reference detector 4 is shown.

11

Table 1: y residual widths (in μm) of all detectors (R = reference detector and T = tested detector) according to different configurations (R = reference detector and T = tested detector). The detectors are labeled as in Fig. 3.

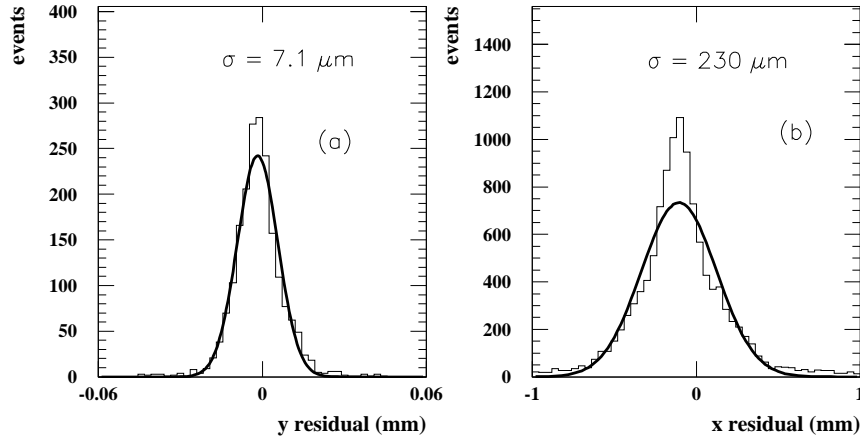| configuration	det. 6	det. 5	det.1	det. 2	det. 3	det. 4
initial (1)	T 17.5	T 18.0	R 3.0	R 2.9	R 2.5	R 2.6
(2)	T 7.1	R 3.7	R 4.3	T 8.1	R 2.6	R 2.6
(3)	R 2.7	T 7.1	R 4.8	T 8.2	R 2.4	R 2.6
(4)	R 2.5	R 2.6	R 2.7	R 2.4	T 31.4	T 31.6
(5)	T 8.5	R 4.0	R 3.5	R 3.8	R 2.8	R 2.7
(6)	R 3.8	T 7.7	R 3.6	R 3.7	R 2.7	R 2.7

Figure 9: Distribution of (a) y residuals and (b) x residuals of the tested detectors 5 and 6. Fitting these distributions with a gaussian function gives the reported residual widths.

5.4.2 Multiple scattering and spatial resolution

Multiple scattering of traversing particles is obtained by considering all materials and detectors that are present in the detector telescope. In addition to the detectors mentioned in Fig.3, three diamond detectors were also inserted, and their contribution in the multiple scattering has also to be considered.

The contribution of the multiple scattering to the resolution, described in details in reference [5], was found here equal to: σ_{ms}=3.2 μm.

The x and y spatial resolution, given by equation 7, are: $\sigma_y = 6.3$ μm and $\sigma_x = 230$ μm.
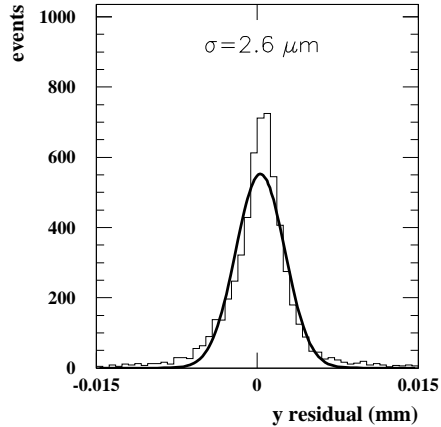
Figure 10: y residual distribution of reference detector 4. Fitting this distribution with a gaussian function gives the indicated residual width.

5.5 Influence of the particle incident angle

A study of the track incident angle variations on the spatial resolution may be performed by considering two possible rotation angles: the first consists of a rotation of the detector around an axis parallel to the strip direction and the second of a rotation around an axis perpendicular to it but in the strips plane. These angles will be denoted $\theta_{//}$ and $\theta_{\perp}$, respectively, in this paragraph.

Variations of $\theta_{//}$ are expected to lead to additional exposed strips than for normal incidence. The resolution is thus expected to be degraded in this case. Variations of $\theta_{\perp}$ are expected to yield less important electron-hole diffusion and should not affect much the resolution.

The effects due to the variations of these two angles on the mean number of strips per cluster have been studied by using the ^{90}Sr source. Only $\theta_{\perp}$ was examined with the pion beam.

With the ^{90}Sr source, the strips of the two detectors under study are oriented orthogonally (see paragraph 2.2), so that the global rotation of the two detectors between 0° and 30° calls for $\theta_{//}$ and $\theta_{\perp}$ changes. The resulting mean numbers of strips per cluster for different angle values are given in table 2. It shows, as expected, a stronger influence of $\theta_{//}$ than of $\theta_{\perp}$ on the variation of the mean number of strips per cluster.

Table 2: Number of strips per cluster for different values of $\theta_{//}$ and $\theta_{\perp}$ by using the ^{90}Sr source.

$\theta_{//}$ (deg)	number of strips per cluster	$\theta_{\perp}$ (deg)	number of strips per cluster
0	3.09	0	2.72
10	3.41	10	2.75
20	4.21	20	2.83
30	5.29	30	3.08

The number of strips per cluster for $\theta_{//} = 0°$ and 30° is also shown in Fig.11.

13
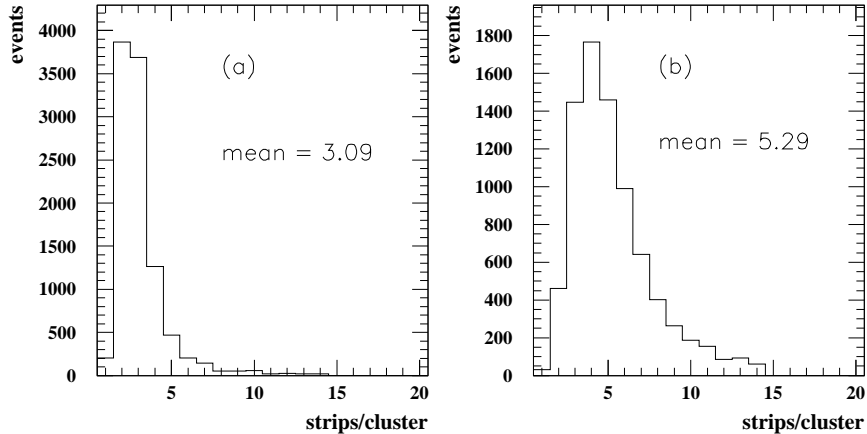
Figure 11: Distribution of the number of strips per cluster by using the ^{90}Sr source, for (a) $\theta_{//} = 0°$ and (b) $\theta_{//} = 30°$.

The influence of the $\theta_\perp$ angle on the mean number of strips per cluster with the pion beam is shown in table 3 and supports, as expected, small variations.

Table 3: Number of strips per cluster for the tested detectors 5 and 6 for different values of the angle $\theta_\perp$.

$\theta_\perp$ (deg)	detector 5	detector 6
0	2.40	2.20
15	2.44	2.31
30	2.45	2.31
45	2.50	2.34

6 Summary and outlook

In this study, we have shown how to extract the physics signal from strips of silicon microstrip detectors exposed to the passage of particles. This allowed a selection of strip clusters and their centroid determination. The used criteria to make this selection have been discussed.

The procedure to measure the x and y resolution of single-sided silicon microstrip detectors has been described. The different steps of the prealignment, the tracking procedure and the alignment of detectors have been presented. The relevance of the detector configuration was also discussed. With the used configuration, y and x residual widths of 7.1 and 230 μm are obtained for both detectors. The contribution of the multiple scattering was determined to be 3.2 μm. The y and x resolutions are thus equal to 6.3 μm and 230 μm. Finally, different incident angles were considered and their effect on the variation of the number of strips per cluster was studied.

Further studies about geometrical effects like incident angle changes (like rotation around the axis parallel to the strip direction) are under way. It remains also essential to compare the results obtained in this work for single-sided detectors with those relative to double-sided detectors. This comparison is currently in progress.

14

References

[1] ALICE Technical Proposal, CERN/LHCC 95-71, LHCC/P3, December 1995

[2] M. Monteno, ALICE Note/SIL/94-13

[3] *Development and application of semiconductor tracking detectors*, ed. by T. Ohsugi, Y. Unno and N. Tamura, Nucl. Inst. and Meth. in Phys. Res. A383 (1996) 349-361

[4] R. Turchetta, Thèse de l'Université Louis Pasteur, Strasbourg, CRN/HE 91-07

[5] G. Lutz, *Optimum track fitting in the presence of multiple scattering*, Nucl. Inst. and Meth. in Phys. Res. A273 (1988) 349-361

[6] C. Colledani et al., Nucl. Inst. and Meth. in Phys. Res. A372 (1996) 379-384